Anti-vascular endothelial growth factor acts on retinal microglia/macrophage activation in a rat model of ocular inflammation

Aude Couturier, Elodie Bousquet, Min Zhao, Marie-Christine Naud, Christophe Klein, Laurent Jonet, Ramin Tadayoni, Yvonne de Kozak, Francine Behar Cohen

Molecular Vision 2014; 20:908-920 <http://www.molvis.org/molvis/v20/908>
Received 29 July 2013 | Accepted 20 June 2014 | Published 23 June 2014

Anti-vascular endothelial growth factor acts on retinal microglia/macrophage activation in a rat model of ocular inflammation

Aude Couturier,[1] Elodie Bousquet,[1,4] Min Zhao,[1] Marie-Christine Naud,[1] Christophe Klein,[2] Laurent Jonet,[1] Ramin Tadayoni,[3] Yvonne de Kozak,[1] F. Behar-Cohen[1,5]

[1]Inserm, U1138, Team 17, Physiopathology of ocular diseases : Threrapeutic innovations, Université René Descartes Sorbonne Paris Cité, Centre de Recherche des Cordeliers, Paris, France; [2]Inserm, U1138, CICC, Université René Descartes Sorbonne Paris Cité, Université Pierre et Marie Curie Paris Centre de Recherche des Cordeliers, Paris, France; [3]Assistance Publique Hôpitaux de Paris, Hôtel-Dieu de Paris, department of Ophthalmology, Hôpital Lariboisière, Paris, France; [4]Assistance Publique Hôpitaux de Paris, Hôtel-Dieu de Paris, department of Ophthalmology, Hôpital Hôtel-Dieu, Paris, France; [5]Department of Ophtahlmology of Lausanne University, Jules Gonin Ophthalmic hospital, Lausanne, Switzerland

Purpose: To evaluate whether anti-vascular endothelial growth factor (VEGF) neutralizing antibodies injected in the vitreous of rat eyes influence retinal microglia and macrophage activation. To dissociate the effect of anti-VEGF on microglia and macrophages subsequent to its antiangiogenic effect, we chose a model of acute intraocular inflammation.
Methods: Lewis rats were challenged with systemic lipopolysaccharide (LPS) injection and concomitantly received 5 µl of rat anti-VEGF-neutralizing antibody (1.5 mg/ml) in the vitreous. Rat immunoglobulin G (IgG) isotype was used as the control. The effect of anti-VEGF was evaluated at 24 and 48 h clinically (uveitis scores), biologically (cytokine multiplex analysis in ocular media), and histologically (inflammatory cell counts on eye sections). Microglia and macrophages were immunodetected with ionized calcium-binding adaptor molecule 1 (IBA1) staining and counted based on their differential shapes (round amoeboid or ramified dendritiform) on sections and flatmounted retinas using confocal imaging and automatic quantification. Activation of microglia was also evaluated with inducible nitric oxide synthase (iNOS) and IBA1 coimmunostaining. Coimmunolocalization of VEGF receptor 1 and 2 (VEGF-R1 and R2) with IBA1 was performed on eye sections with or without anti-VEGF treatment.
Results: Neutralizing rat anti-VEGF antibodies significantly decreased ocular VEGF levels but did not decrease the endotoxin-induced uveitis (EIU) clinical score or the number of infiltrating cells and cytokines in ocular media (interleukin [IL]-1β, IL-6, tumor necrosis factor [TNF]-α, and monocyte chemoattractant protein [MCP]-1). Eyes treated with anti-VEGF showed a significantly decreased number of activated microglia and macrophages in the retina and the choroid and decreased iNOS-positive microglia. IBA1-positive cells expressed VEGF-R1 and R2 in the inflamed retina.
Conclusions: Microglia and macrophages expressed VEGF receptors, and intravitreous anti-VEGF influenced the microglia and macrophage activation state. Taking into account that anti-VEGF drugs are repeatedly injected in the vitreous of patients with retinal diseases, part of their effects could result from unsuspected modulation of the microglia activation state. This should be further studied in other ocular pathogenic conditions and human pathology.

Microglial cells, the main resident sentinel immune cells, are located around vessels in the inner part of the healthy retina [1-6]. In diabetic retinopathy [7,8], age-related macular degeneration (AMD) [9], uveitis [10], and aging [11-13], these cells become activated and may migrate in the sub-retinal space [13]. The migration and activation of microglia are often a non-specific early stress response. Hyperglycemia-induced glial activation has been suspected to contribute to the early development of diabetic retinopathy and is associated with electroretinographic alterations before any signs of microangiopathy are clinically detectable [14,15]. In experimental uveitis or in light-induced retinal damage, resident microglia migrate toward the photoreceptor cell layer where they generate tumor necrosis factor-alpha (TNF-α) and peroxynitrite witnessing nitric oxide (NO) production and inducible nitric oxide synthase (iNOS) activation, before the circulating macrophages and polymorphonuclear cells infiltrate the eye tissue [10]. The cytokines and toxic mediators (such as NO) released by activated microglia under these conditions are suspected to be neurotoxic to photoreceptor cells [16-19] suggesting that activation of microglia may contribute to permanent retinal damage. However, retinal microglia constitutively secrete interleukin-27 (IL-27), and its expression is upregulated during uveitis. IL-27 signaling then induces the production of anti-inflammatory molecules by photoreceptor cells such as IL-10 and suppressor of cytokine signaling 1 (SOCS1), suggesting that microglia could also control the inflammatory response [20]. Microglia, depending on its activation state, is a key and early regulator

Correspondence to: Francine Behar-Cohen, 15 rue de l'Ecole de Médecine 75006 Paris, Phone: 0033140467840; FAX: 0033140467840; email: francine.behar-cohen@crc.jussieu.fr

in retinal inflammation and a potential modulator of the inflammatory response.

The exact molecular events that trigger microglia activation remain imperfectly understood. Chemokines, and CX3CR1 (receptor for CX3C chemokine ligand 1; CX3CL1) in particular, have shown to control microglia migration in the retina since CX3CR1 knockout (KO) mice show spontaneous microglia accumulation in the sub-retinal space and subsequent photoreceptor degeneration [9]. In humans, the CX3CR1 polymorphism may be associated with wet AMD risk [9].

More recently, we have shown that in a non-obese type 2 diabetic rat, retinal microglia accumulation in the sub-retinal space could result from impaired transepithelial migration of microglia through intact RPE cells in hyperglycemic conditions. In the normal retina, and more intensively with aging, transcellular pores have been identified in the RPE, which could contribute to microglia trafficking between the retina and the choroid [13]. Hyperglycemia could impair this physiologic trafficking contributing to sub-retinal activated microglia accumulation and subsequent retinal damage.

During endotoxin-induced uveitis (EIU), myeloid cells differentially infiltrate tissues of the anterior and posterior segments of rat eyes. In the iris, infiltration of monocytes is observed as early as 2 h after lipopolysaccharide (LPS) injection, followed by massive myeloid cell infiltration, mostly polymorphonuclear, at 4–6 h. The number of cells with dendritic shape decreases by about 50% at 24 h [21]. In the retina, resident macrophages and microglia migrate and aggregate around retinal blood vessels at 4 h. At 16 h, when uveitis is clinically detectable, a more massive infiltration of macrophages with round, pleiomorphic, and dendritiform shapes is observed, followed after 72 h and thereafter by a predominant dendritiform cells morphologic change all over the retina [22]. The chemical depletion of the circulating macrophages has given some insight into their pathogenic role during EIU. Although significantly decreased cell infiltration was observed in the anterior segment, retinal and choroidal cell infiltration was not decreased, suggesting that monocyte infiltration plays a minor role in retinal inflammation during EIU [23]. Interestingly, monocytes and macrophages are now viewed as important but complex actors in the pathogenesis of age-related macular degeneration [24].

Human monocytes and macrophages express Flt-1 [25], and murine brain microglial cells were shown to express in vitro, vascular endothelial growth factor (VEGF) receptor 1 (VEGF-R1, Flt-1) but not VEGF-R [26]. In a model of traumatic brain injury, intracerebral injection of VEGF induced the invasion of activated microglia in the injured site at day 5 that persisted up to day 60 [27], suggesting that VEGF may be involved in recruiting and activating microglia. In a neurodegeneration model induced by intracerebral injection of the amyloid-β-peptide, Flt-1 was shown to mediate VEGF-induced microglial migration and activation, suggesting a functional role for Flt-1 in mediating the microglial chemotactic inflammatory response that contributes to pathological conditions in Alzheimer disease [28].

Whether anti-VEGF drugs commonly used in ocular conditions associated with VEGF increase could modulate retinal microglia and macrophage activation has not been examined. Anti-VEGF drugs are routinely used in treating wet AMD to reduce deleterious consequences of choroidal neovascularization [29-31]. In other ocular diseases, anti-VEGF drugs efficiently reduced macular edema secondary to vein occlusion [32] and diabetic retinopathy [33,34]. Interestingly, the chronic use of anti-VEGF for diabetic macular edema was shown to exert unexpected beneficial effects on the development and severity of diabetic retinopathy, but the mechanism of this clinical effect remains unclear [35].

We have hypothesized that anti-VEGF treatments could exert direct effects on microglia activation and migration in the retina. To explore this hypothesis, we have evaluated the effect of a specific rat anti-VEGF antibody, administered via an intravitreous route, on migration and activation of rat microglia in an acute model of intraocular inflammation, EIU. EIU is induced by systemic injection of LPS [36], a known activator of retinal microglia [37].

Although anti-VEGF did not influence the severity of uveitis, the treatment induced a strong inhibitory effect on retinal and choroidal microglia activation. This result suggests that anti-VEGF treatments may have indirect unsuspected effects on retinal diseases by inhibiting microglia activation.

METHODS

Animal model: All experiments were performed in accordance with the ARVO Statement for the Use of Animals in Ophthalmic and Vision Research and European Communities Council Directive 86/609/EEC. Experiments were submitted and approved by the ethic committee of Paris Descartes University (number: Ce5/2012/123), The care and use of the animals was in compliance with ARVO statement for the Use of Animals in Ophthalmic and Vision Research. Accreditation N° of the laboratory: B 75 06 02. Adult female Lewis rats (6–8 weeks old; Janvier, Le Genest-Saint-Isle, France) were used for in vivo experiments. The rats were anesthetized with intraperitoneal injection of pentobarbital (25 mg/kg Nembutal; Abbot, Saint-Remy sur Avre, France). Rats were killed by a lethal dose of pentobarbital intraperitoneal

injection. At least 20 animals per treatment group and 20 untreated controls or control immunoglobulin G (IgG) were used, and the experiments were repeated twice. EIU was induced in rats with a single footpad injection of 100 µl sterile pyrogen-free saline containing 200 µg LPS from *Salmonella typhimurium* (Sigma-Aldrich, Saint Quentin Fallavier, France) [38].

Animals were examined with slit-lamp at 24 h, the clinical peak of the disease in our experiments, and at 48 h. The intensity of the clinical ocular inflammation was scored on a scale from 0 to 5 for each eye, as described previously [38]: grade 0: no inflammation; grade 1, minimal iris and conjunctival vasodilation but without cells in the anterior chamber; grade 2, moderate iris and conjunctival vessel dilation but without evident cells in the anterior chamber; grade 3, intense iris vessels dilation and fewer than 10 cells per slit-lamp field in the anterior chamber; grade 4, more severe clinical signs than grade 3, with more than ten cells in the anterior chamber with or without the formation of hypopion; grade 5, intense inflammatory reaction, fibrin formation in the anterior chamber, and total seclusion of the pupil. Clinical evaluation was performed in a masked manner.

Treatments: Intravitreous injections were performed using microfine (300 µl) syringes with 30G needles under topical anesthesia (tetracaine 1%; Sigma-Aldrich). Intravitreous injections of 5 µl anti-VEGF (rat VEGF antibody, RnD system, Lille, France, at 1.5 mg/ml) or vehicle (PBS; 1X 4.3 mM Na_2HPO_4, 137 mM NaCl, 2.7 mM KCl, 1.8 mM KH_2PO_4) or rat IgG isotype, RnD System, Lille, France at 1.5 mg/ml) were performed in the rat eyes at the time of LPS challenge. The final vitreous concentration was chosen similar to the bevacizumab final concentration commonly used in the clinic (1.25 mg in 8 ml, 0.15/ml). Rats were sacrificed by a lethal dose of pentobarbital at either 24 or 48 h after injections.

The first experiment was performed with the rat isotype IgG antibody, which is the real control to ensure that any observed effect is not related to the protein itself but rather due to the specific anti-VEGF activity. For this experiment, rats were treated with either the vehicle or the IgG isotype antibody at the time of LPS injection (five rats/ten eyes per group), and they were euthanized at 24 h to quantify the activated microglia on eye cryosections. Since the isotype IgG did not exert an effect, either on inflammation or on microglia activation, we then performed all other experiments with the vehicle as the control.

Polymorphonuclear cell quantification: Polymorphonuclear cells, identified by the shape of their nuclei stained with 4',6-diamidino-2-phenyl-indole (DAPI), were quantified on histologic sections. The analysis was performed on five eyes per experimental group, with six sections per eye at the optic nerve head level. Results are expressed as mean ± standard deviation (SD). Digitized micrographs were obtained using a digital camera (Spot; BFI Optilas, Evry, France).

Sample collection: Aqueous humor and vitreous were collected and pooled from each enucleated eye to get enough ocular media for multiplex analysis. Ocular media refers to the mixed aqueous humor and vitreous from a single eye. Ocular fluids were immediately centrifuged. The cell-free fractions were collected and frozen at −20 °C before analysis with multiplex assay. Neuroretinas were carefully dissected from the enucleated eyes, snap frozen, and stored at −80 °C until use for RT–PCR analyses. For immunohistochemistry, eyeballs were collected and fixed for 1 h at room temperature in PBS containing 4% paraformaldehyde before they were rinsed overnight in PBS. The next day, the samples were embedded and frozen in optimal cutting-temperature (OCT) compound (Tissue-Tek; Sakura Finetek, Zoeter-woude, the Netherlands) and stored at −80 °C. Cryosections (10 µm thick) of eyes were performed at the optic nerve level using a cryostat (CM 3050S; Leica, Rueil-Malmaison, France) and mounted on slides (Superfrost; Gerhard Menzel, Brauschweig, Germany) for immunohistochemical analysis.

Chemokine and cytokine multiplex assay: Intraocular fluids were subjected to multiplex bead analysis [38]. This method uses microspheres as the solid support for immunoassays and allows the titration of a greater number of cytokines with increased sensitivity than occurs with enzyme-linked immunosorbent assay (ELISA). For each sample, 17 analytes were quantified simultaneously using the rat cytokine/chemokine-17 plex kit (Milliplex Map Kit; Millipore, Saint-Quentin-en-Yvelines, France) according to the manufacturer's instructions, as follows: chemokines monocyte chemoattractant protein (MCP)-1/CCL2, MIP-1α/CCL3, RANTES/CCL5, IP10/CXCL10 (IFN-inductible protein-10) and GRO/KC; proinflammatory mediators IL-1β, IL-8, and TNF-α; Th1/Th2/Th17 cytokines IL-2 and IFN-γ /IL-4, IL-5, IL-6, Il-10, and IL-13/IL17. The assay was performed in a 96-well filter plate, and standard curves for each cytokine were generated with the rat cytokine standard provided in the kit. All incubation steps were performed under medium orbital agitation in the dark to protect the beads from light. Data acquisition and analysis were performed with the manager software version 4.1 (Bioplex; Bio-Rad) with five logistic parameters for standard curves. Detection thresholds for all analytes were estimated to be approximately 1 to 10 pg/ml.

Reverse transcription and real-time PCR: Total RNA was isolated from neuroretinas from anti-VEGF and vehicle-injected EIU rat eyes (n = 5 eyes of five rats per group;

RNeasy Plus Mini Kit; Qiagen, Courtaboeuf, France). First-stand cDNA was synthesized using random primers (Invitrogen, Cergy Pontoise, France) and reverse transcriptase (Superscript II; Invitrogen). Transcript levels of nitric oxide synthase 2 (NOS2) and TNF-α were analyzed with real-time PCR performed in a real-time PCR system (7500 Real-Time PCR System; Applied Biosystems, Foster City, CA) with either SYBR Green (for NOS2) or TaqMan (for TNF-α) methodology. RT-qPCR reactions were carried out with 100 ng cDNA sample. Non-template control reactions were performed for each gene, in order to assure nonspecific amplification. Reactions were performed with the following thermal profile: 10 min. at 95°C plus 40 cycles of 15 seconds at 95°C and 1 min. at 60°C. Real-time PCR results were analyzed with SDS 2.1 software (Applied Biosystems) and quantification were calculated on the basis of threshold cycle (C_T) for the target gene and the reference gene 18S according to the following formula: 2 $\Delta(C_T(GADPH) - C_T(Target))$.The 18S was used as an internal control. The delta cycle threshold calculation was used for relative quantification of the results.

Immunofluorescence: Microglial cells were visualized with immunofluorescence, using rabbit polyclonal anti-ionized calcium binding adaptor molecule 1 (anti-IBA1; 1:400, Wako, Richmond, VA), a specific marker for microglia and macrophages [39]. To evaluate microglial cell activation, NOS2 expression was visualized using a mouse monoclonal anti-NOS2 (1:100; Santa Cruz Biotechnology, Heidelberg, Germany). Expression of VEGF-R1 and VEGF-R2 was evaluated with coimmunostaining with IBA1.

Briefly, after permeabilization with 0.1% Triton X-100 in PBS for 30 min, specimens were rinsed and saturated for 30 min with 5% goat serum in PBS. They were incubated overnight at 4 °C with the primary antibodies. After washing, sections were incubated for 1 h at room temperature with a secondary Alexa Fluor 488 (green)-conjugated goat anti-rabbit monoclonal antibody and a secondary Alexa Fluor 594 (red)-conjugated goat anti-mouse monoclonal antibody, each at dilution 1:200 (Invitrogen). For each step, antibodies were diluted in PBS-1% goat serum. After the nuclei were stained with DAPI (1:5,000; Sigma-Aldrich), the sections were mounted with gel mount and were observed with a fluorescence laser scanning microscope (Olympus BX51, Rungis, France).

Quantification of activated ionized calcium-binding adaptor molecule 1–stained cells: To quantify microglial activation and migration, IBA1 round amoeboid cells were counted on six retina and choroid 7 µm sections at the optic nerve level (and on five eyes per treatment group). Cell number was expressed as the mean ± standard deviation (SD) of the total cells per section.

Retinal flatmounting: Eyes were fixed for 15 min in 4% paraformaldehyde (Ladd Research Industries, Inland Europe, Conflans-sur-Lanterne, France). After being washed, the retinas were isolated, cut into four orthogonal incisions, and postfixed with acetone 100% at −20 °C for 15 min. They were then rehydrated with PBS containing 1% Triton X-100, and incubated with the rabbit anti-IBA1 antibody (1:400) at room temperature under stirring overnight. After being washed with PBS, the Alexa Fluor 488-conjugated goat anti-rabbit IgG (1:200; Molecular Probes, Leiden, the Netherlands) was applied for 1 h. The retinas were flatmounted using gel mount with the vitreous side up. Images were taken using a fluorescence laser scanning microscope (Olympus BX51, Rungis, France) and a confocal laser scanning microscope (Zeiss LSM 710; Carl Zeiss MicroImaging, Oberkochen, Germany). Confocal microscopic images spanning the full thickness of the retina were performed by scanning at 1 µm increments (objective 20X lens). The total IBA1 immunostained area was quantified on flatmounted images, using automatic measurements of the IBA1 surface (ImageJ). A specific macro was built to distinguish between the round IBA1 staining area and the total IBA1 staining area. To confirm that this program adequately distinguished round amoeboid IBA1-positive cells, we correlated automated drawing of round cells and amoeboid and IBA1-positive cells to manual counts on two areas (of 1 mm^2) of five retinas (by two independent observers). The correlation coefficient was 98%. This method was therefore used to quantify IBA1 staining on eight regions (of 1 mm^2) from the different quadrants of the retina (two per quadrants).

Statistical analysis: Data are expressed as mean ± standard error of the mean (SEM). Statistical analysis was conducted using a software program for predictive analytics (GraphPad Prism 5; GraphPad Software, San Diego, CA). The Mann–Whitney test was used when two groups were compared. Values of $p<0.05$ were considered significant.

RESULTS

Vascular endothelial growth factor neutralization does not exert an anti-inflammatory effect on endotoxin-induced uveitis: Intravitreous injection of rat anti-VEGF antibody at the time of the LPS challenge did not influence the clinical uveitis score at 24 h (2.6±0.2) or at 48 h (1.7±0.1) compared to vehicle injection (2.8±0.1 and 1.80±0.4 at 24 and 48 h, respectively, n = 5 rats per group, $p>0.05$; Figure 1A). Rat anti-VEGF significantly reduced ocular VEGF levels at 24 h from 16.7±5 pg/ml to 3.36±1.3 pg/ml in rat ocular media (n = 5 rats per

group, p = 0.0436; Figure 1B) validating its expected biologic effect, but did not reduce the severity or duration of EIU in rats. Rat isotype IgG did not exert an anti-inflammatory effect and did not reduce ocular VEGF (data not shown). In agreement with clinical scoring, cytokines, measured in the ocular media of rats at either 24 or 48 h after LPS injection using multiplex, did not vary significantly in the group of rats treated with anti-VEGF compared to the vehicle-treated rats. In particular, the IL-1β level was measured at 130.9±48.99 pg/ml in the anti-VEGF group versus 99.54±11.34 pg/ml in the vehicle group, p = 0.5501; IL-6 3587±493.9 pg/ml in the anti-VEGF group versus 4879±560.1 pg/ml in the vehicle group, p = 0.1266; TNF-α was 21.46±4.35 pg/ml in the anti-VEGF group versus 27.36±2.45 pg/ml in the vehicle group, p = 0.3090; MCP-1 was 9854±1239 pg/ml in the anti-VEGF group versus 10,596±374.7 pg/ml in the vehicle group, p = 0.6226). At 48 h, ocular cytokines decreased similarly in both groups (data not shown; IL-1β was 23.43±7.24 pg/ml in the anti-VEGF group versus 28.63±18.50 pg/ml in the vehicle group, p = 0.8003; IL-6 171.8±51.70 pg/ml in the anti-VEGF group versus 410.3±107.2 pg/ml in the vehicle group, p = 0.0685; TNF-α was 6.87±1.59 pg/ml in the anti-VEGF group versus 7.50±0.69 pg/ml in the vehicle group, p = 0.7273; MCP-1 was 2853±667.2 pg/ml in the anti-VEGF group versus 3899±706.8 pg/ml in the vehicle group, p = 0.3132).

In agreement with the cytokine levels and clinical scoring, at 24 h, the number of polymorphonuclear cells infiltrating the ocular tissues did not differ significantly in eyes treated with vehicle (14.9±2.1 cells/section, n = 5), compared with eyes treated with anti-VEGF (13.3±3.5 cells/section, n = 5, p>0.05; Figure 1C). All together, these results show that neutralizing VEGF does not exert an anti-inflammatory effect on EIU.

Vascular endothelial growth factor neutralization reduces the number of round activated microglia in endotoxin-induced uveitis: Activation of microglia induces modification of its shape from ramified multidirectional extensions to polarized dendrites and then to round amoeboid cells (Figure 2A,D inset). The number of activated round amoeboid microglia did not vary significantly in eyes treated with the rat IgG isotype antibody compared to the vehicle-treated eyes (n = 5 rats per group, p>0.05; Figure 2H). However, in the eyes treated with anti-VEGF at 24 h compared to the vehicle-injected eyes, the number of round amoeboid IBA1-positive cells was significantly decreased in the inner retina (18.42±1.35 cells/section in the inner retina compared to 39±0.5 cells/section, n=5 rats per group, p<0.0001), the outer retina (2.2±0.5 cells/section as compared to 9±1.8 cells/section, n = 5 rats per group, p<0.001), and the choroid (41±2.5 cells/section compared to 56±6 cells/section, n = 5 rats per group, p<0.05; Figure 2A-G). At 48 h, although numerous activated cells were still present in the retina and the choroid of rats with EIU, the IBA1-positive cells could hardly be identified in the anti-VEGF-treated rats (not shown). The morphology of IBA1-positive cells was also

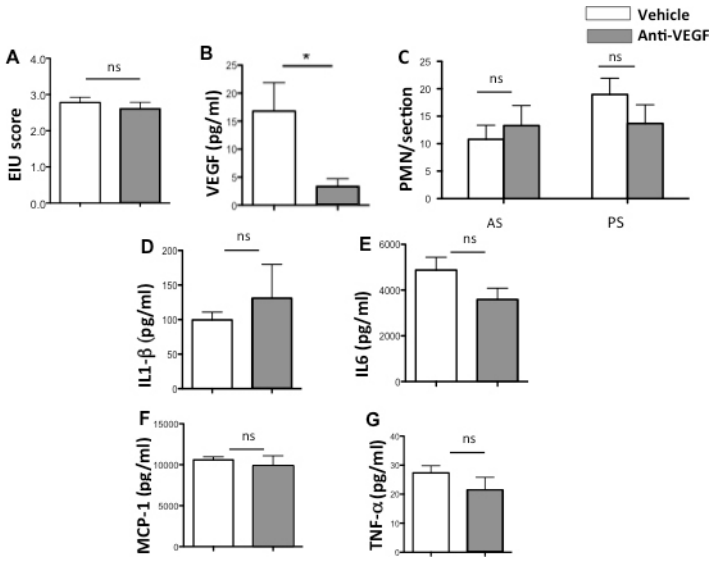

Figure 1. Clinical and biological effects of anti-VEGF on EIU in rats. **A**: Clinical scoring of endotoxin-induced uveitis (EIU; n = 5 rats per group, p>0.05). **B**: vascular endothelial growth factor (VEGF) ocular levels (pg/ml) at 24 h (n = 5 rats per group, p = 0.0436). **C**: Polymorphonuclear cell infiltration in the anterior segment (AS) and in the posterior segment (PS) of rats (five sections/ eye, five eyes per group). **D**: Ocular levels of interleukin (IL)1-β (πγ/μλ; n = 5, p = 0.55), **E**: IL-6 (pg/ml; n = 5, p = 0.068). **F**: Monocyte chemoattractant protein-1 (MCP-1; pg/ml; n = 5, p = 0.3132). **G**: Tumor necrosis factor (TNF)-α (πγ/μλ; n = 5, p = 0.7273).

modified by anti-VEGF treatment in the iris and ciliary body (not shown) and the choroid (Figure 2D-G), where numerous round cells were observed in the EIU-vehicle-injected eyes compared to the ramified, dendritic IBA1-positive cells in the anti-VEGF-injected eyes. Because quantifying cells on sections may not represent cellular events that occur all over the retina, we also counted IBA1-positive cells on the entire flatmounted retina.

On the flatmounted retinas, numerous round amoeboid microglia were observed in the vehicle-injected EIU rats (Figure 3A–C, arrows), while more ramified cells were observed after anti-VEGF treatment (Figure 3B-D). To count the total number of microglia in the inner neuroretina and the relative number of round and ramified IBA1-positive cells, the surface of the fluorescently stained IBA1-positive cells was analyzed automatically after the different microglia shapes were captured on the flatmounted retina as illustrated in Figure 3C,D. This automated quantification showed that although no significant difference was observed in the total surface of IBA1 staining between the anti-VEGF and

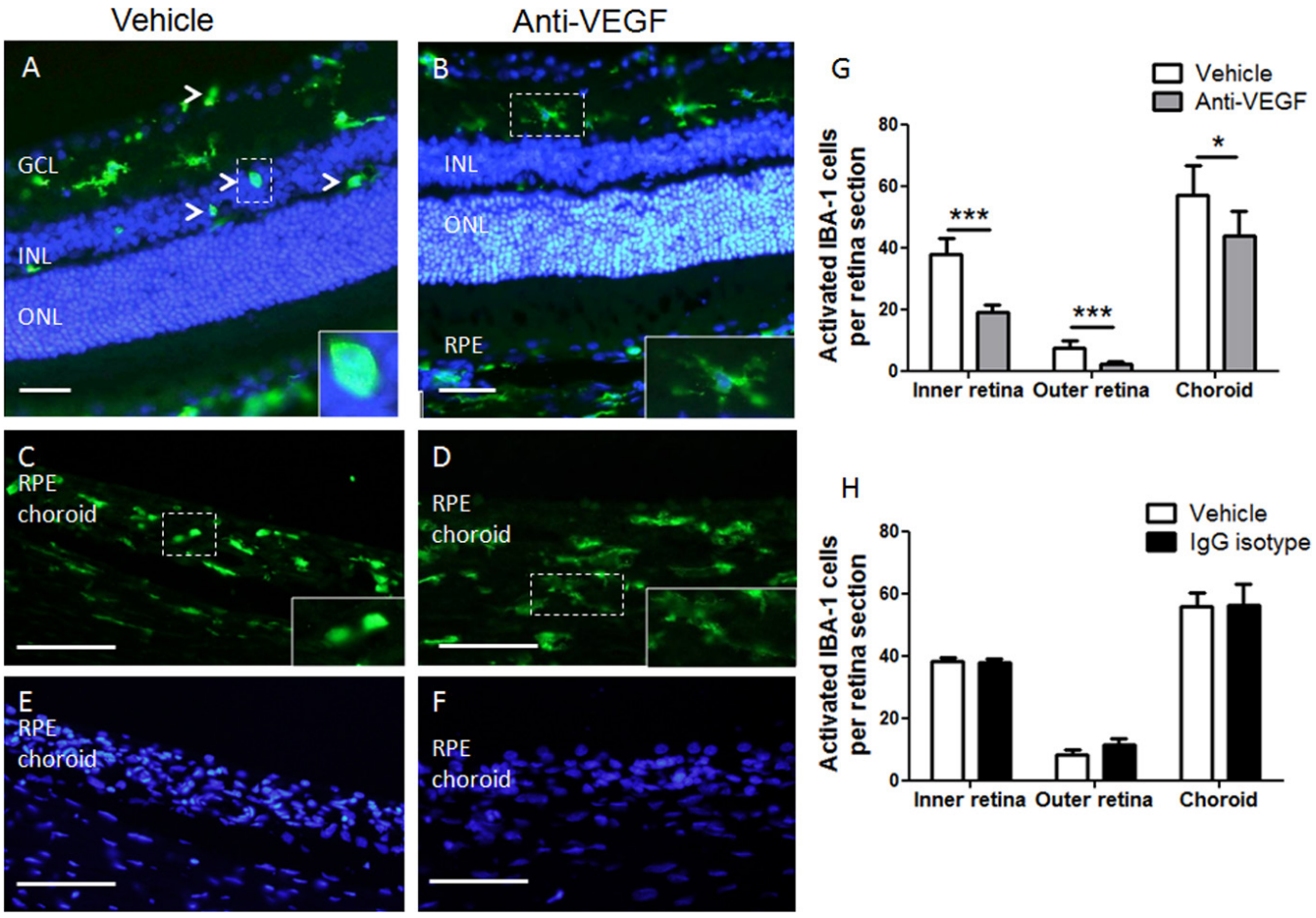

Figure 2. Ionized calcium-binding adaptor molecule 1 immunostaining of microglia and macrophages in endotoxin-induced uveitis at 24 h after lipopolysaccharide injection **A**: Retina section after vehicle intravitreal injection; in green ionized calcium-binding adaptor molecule 1 (IBA1) staining and in blue nuclei are stained with 4',6-diamidino-2-phenyl-indole (DAPI). Arrowheads indicates round IBA1-positive cells, magnified in the inset. Bar = 50 µm, GCL = ganglion cell layer, INL = inner nuclear layer, ONL = outer nuclear layer. **B**: Retina section after anti-vascular endothelial growth factor (VEGF) intravitreal injection. IBA1-positive cells (in green) are ramified and elongated in the inner retina as magnified in the inset. Nuclei are stained in blue with DAPI. Bar = 50 µm, GCL = ganglion cell layer, INL = inner nuclear layer, ONL = outer nuclear layer. **D**–**F**: Choroid section after vehicle intravitreal injection stained with IBA1 (**D**) and DAPI (**F**), showing round amoeboid cells (magnified in the inset). Bar = 50 µm, RPE = retinal pigment epithelial cells. **E**–**G**: Choroid section after anti-VEGF intravitreal injection stained with IBA1 (**E**) and DAPI (**G**), showing round elongated ramified cells (magnified in the inset). Bar = 50 µm, RPE = retinal pigment epithelial cells. **C** and **H**: Quantification of round IBA1-positive cells in the inner and outer retina and in the choroid of rat eyes with EIU at 24 h, injected either with vehicle or with anti-VEGF antibody (**C**) or with control rat isotype immunoglobulin G (IgG) antibodies (**H**) *p<0.05, ***p<0.0001.

vehicle-treated eyes (n = 10 retinas per group, p>0.05), the area of fluorescence resulting from round IBA1 immunolabeled cells was significantly decreased after anti-VEGF treatment compared to the vehicle-treated eyes (n = 10 retinas per group, p<0.05; Figure 3E,F). NOS2 is expressed in activated macrophages and microglia and is a marker of the activation state [13,38]. As shown in Figure 4, double-stained IBA1/NOS2 positive round cells were identified in the retinas of eyes with EIU treated with vehicle (Figure 4A–C), but none were found in the anti-VEGF-treated eyes (Figure 4D-F). NOS2 expression was also decreased at the mRNA levels in the anti-VEGF-treated retinas compared to the vehicle-treated retinas (Figure 4G). TNF-α expression by microglia is also a marker of its activation, but TNF-α expression was not significantly reduced in the whole neuroretina of eyes treated with anti-VEGF compared to controls even if a trend was observed (data not shown).

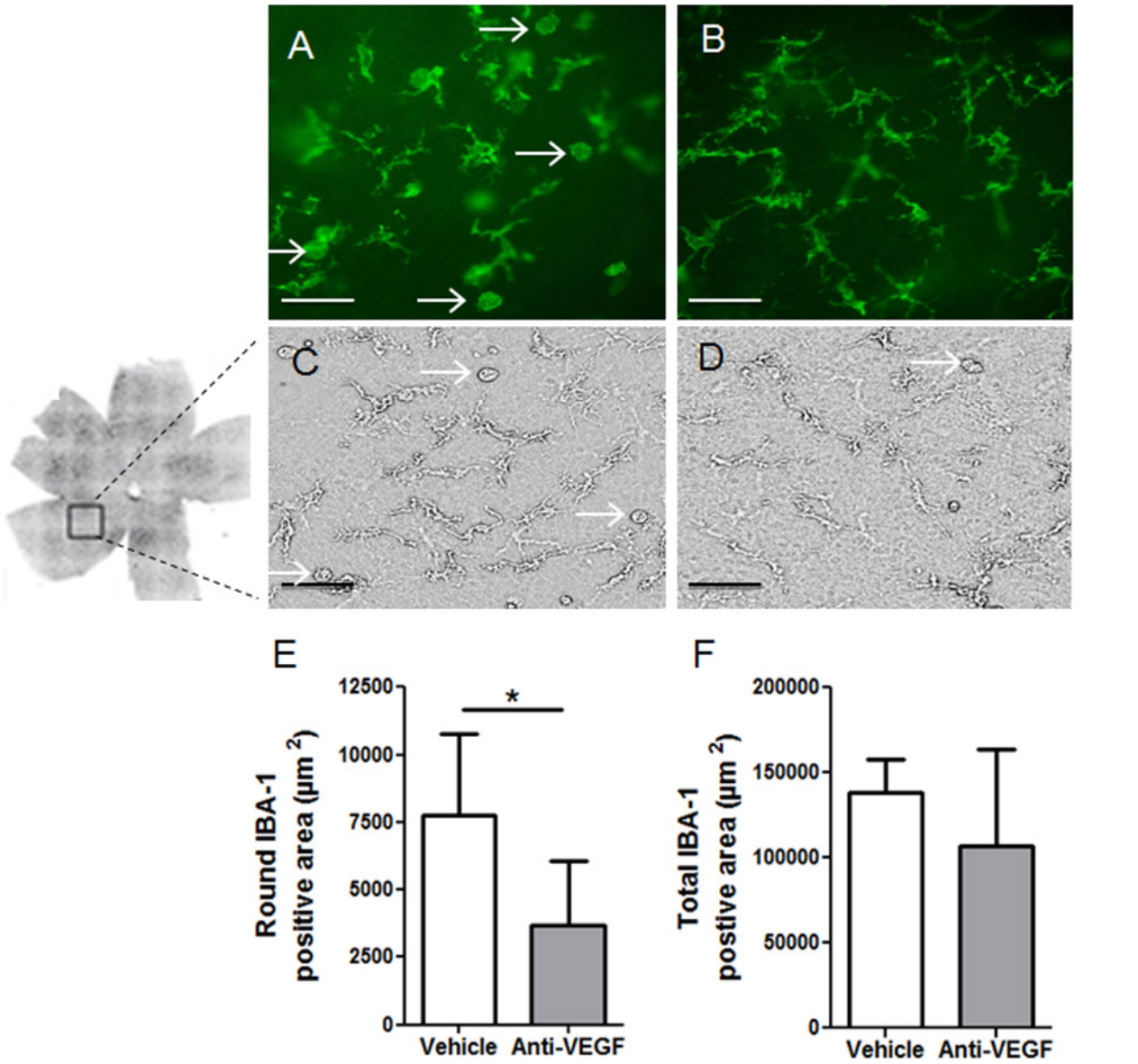

Figure 3. Ionized calcium-binding adaptor molecule 1 immunostaining on flatmounted retinas. **A**–**B**: Example of flatmounted retinas from rat eyes with endotoxin-induced uveitis (EIU) injected with vehicle (**A**) or with antivascular endothelial growth factor (VEGF) antibodies (**B**); Bar = 50 µm. Arrowhead show round reactive ionized calcium-binding adaptor molecule 1 (IBA1)-positive cells. **C**–**D**: Extraction of cell contours used for automatic labeling of IBA1 staining. **E-F**: Quantification of round and total IBA-1 positive cells on flat-mounted retina from EIU control and anti-VEGF treated eyes. Bar = 50 µm.

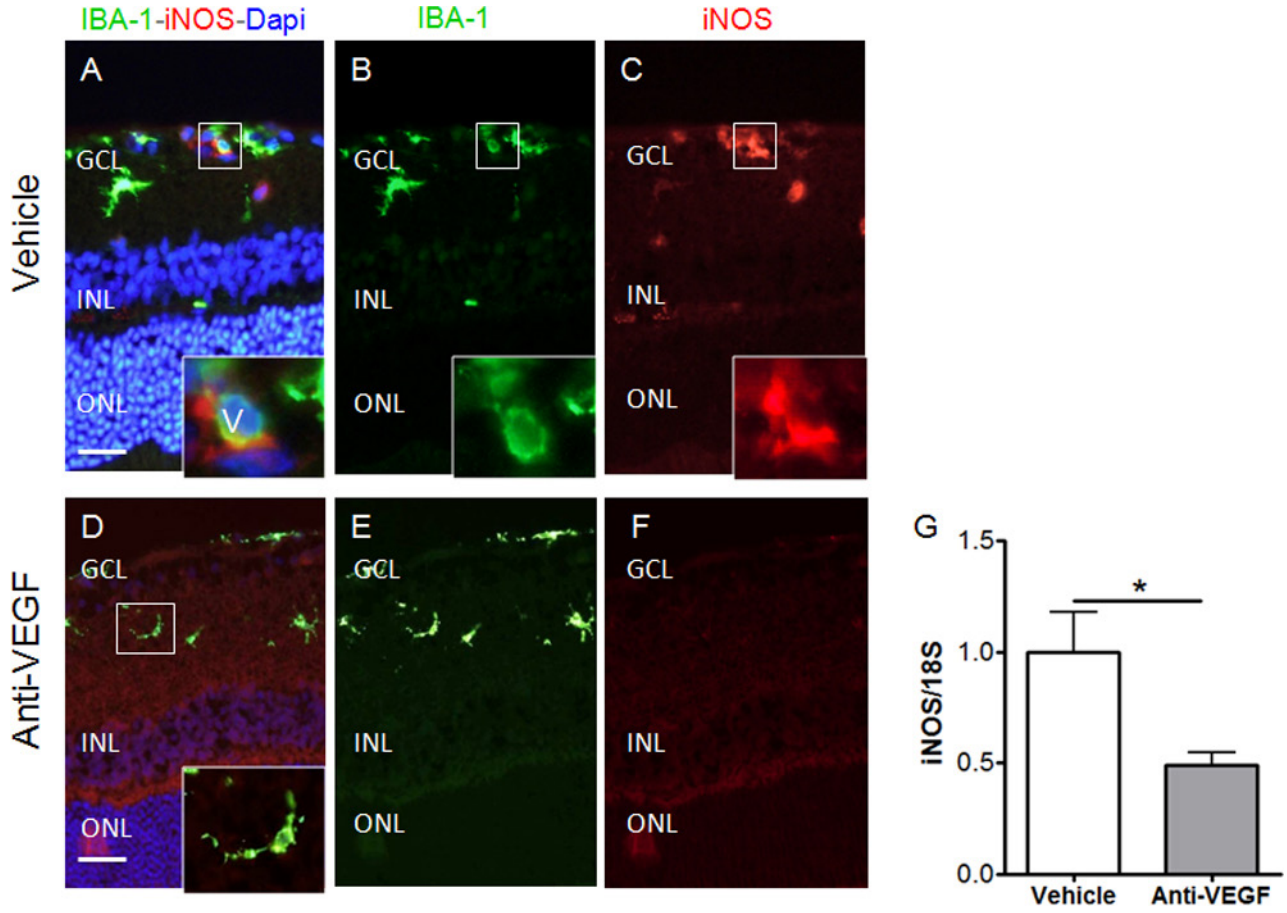

Figure 4. Inducible nitric oxide synthase expression: immunohistochemistry and RT–PCR inducible nitric oxide synthase and ionized calcium-binding adaptor molecule 1 coimmunostaining on retinal sections of rats with endotoxin-induced uveitis injected with vehicle (**A**–**C**) or with antivascular endothelial growth factor (**D**–**F**). **A** and **D**: Ionized calcium-binding adaptor molecule 1 (IBA1) cells are labeled in green, iNOS is labeled in red and nuclei are stained in blue with 4',6-diamidino-2-phenyl-indole (DAPI). **B** and **E**: IBA1 cells labeled in green. **C** and **F**: Inducible nitric oxide synthase (iNOS) labeled in red. GCL = ganglion cell layer, INL = inner nuclear layer, ONL = outer nuclear layer, RPE = retinal pigment epithelial cells, Chor: choroid. Bar = 50 µm. Insets are increased magnifications (5X) of regions delimited by squares. **G**: iNOS mRNA expression on retinal extracts from vehicle and antivascular endothelial growth factor (anti-VEGF) rat eyes; n = 5 per groups * $p<0.05$).

Vascular endothelial growth factor receptor expression in retinal microglia: At 24 h after LPS injection, VEGF receptor expression was evaluated in microglial cells with coimmunostaining of VEGF-R1 or -R2 and IBA1. A subset of IBA1-positive cells expressed VEGF-R1, particularly the round activated ones (Figure 5A-C and inset). In eyes treated with anti-VEGF, VEGF-R1 remained expressed in a subset of IBA1-positive cells (Figure 5D-F). VEGF-R2 was expressed in sparse perivascular IBA1-positive cells (Figure 6A-C and inset). In the anti-VEGF-treated eyes, the expression of VEGF-R2 decreased in deactivated macrophages and microglia (Figure 6D-F).

DISCUSSION

Anti-VEGF drugs used in treating retinal diseases aim at controlling angiogenic processes or vascular leakage that are at least partly VEGF-driven [40]. However, the mechanisms of action of anti-VEGF drugs on various retinal diseases are not fully understood. Sub-clinical inflammation with microglial or macrophage activation has been suspected to contribute to retinal pathogenesis in diabetic retinopathy and age-related macular degeneration [11,24], but the effect of anti-VEGF treatment on retinal microglia and macrophages has not been analyzed independently from an angiogenic context although anti-VEGF drugs were approved for macular edema not related to neovascularization. Importantly, macrophages express VEGFR-1 (Flt-1), and the use of

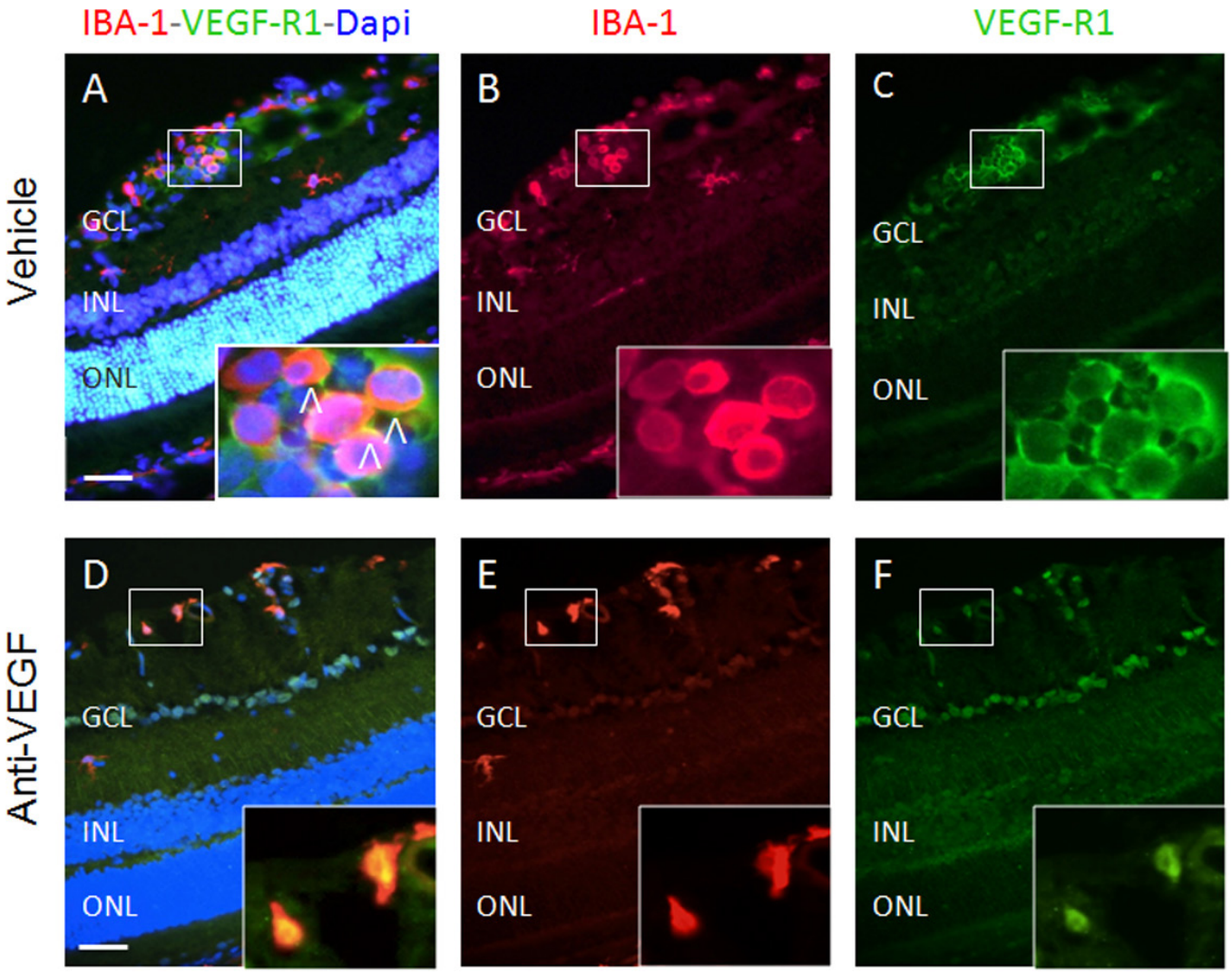

Figure 5. VEGF-R1 and IBA1 co-immunostaining on retinal sections retinal sections of EIU rats injected with vehicle (**A**–**C**) or anti-VEGF (**D**–**F**). GCL = ganglion cell layer, INL = inner nuclear layer, ONL = outer nuclear layer, RPE = retinal pigment epithelial cells, Chor = choroid. Insets are increased magnification (5X) of regions delimited by squares. Bar = 50 µm.

Flt-1-deficient mice demonstrated that in rheumatoid arthritis models, VEGF induced macrophage activation through Flt-1-dependent signaling [41,42]. In the brain, VEGF-induced migration and proliferation of microglia were also shown to result from Flt-1 activation [26], which mediated microglial responses to the amyloid peptide, suggesting its contribution in Alzheimer disease [28].

In the rat retina, we found that microglia and macrophages express Flt-1 (VEGF-R1) in inflammatory conditions in vehicle- and anti-VEGF-treated eyes. However, not all IBA1-positive cells expressed VEGF-R1 suggesting that potentially only a subset of cells is directly VEGF-sensitive. Interestingly, in eyes with EIU, reactive round microglia cells seemed to overexpress VEGF-R1 compared to the inactivated dendritic ones and expressed VEGF-R2. This overexpression of Flt-1 was found in vitro in activated monocytes [43]. Moreover, in a rat model of spinal cord injury, upregulation of VEGF-R1 and VEGF-R2 mRNA occurred in microglia and macrophages that infiltrated the lesion site early, suggesting that in activated conditions both VEGF receptors could be expressed [44].

Macrophages and microglia express VEGF receptors, and have been recognized in the pathogenesis of retinal diseases treated with anti-VEGF. Therefore, we studied the effect of anti-VEGF in an acute model of ocular inflammation in which microglial migration and activation have been previously characterized [45]. This inflammatory non-angiogenic model was chosen to distinguish anti-VEGF effects not

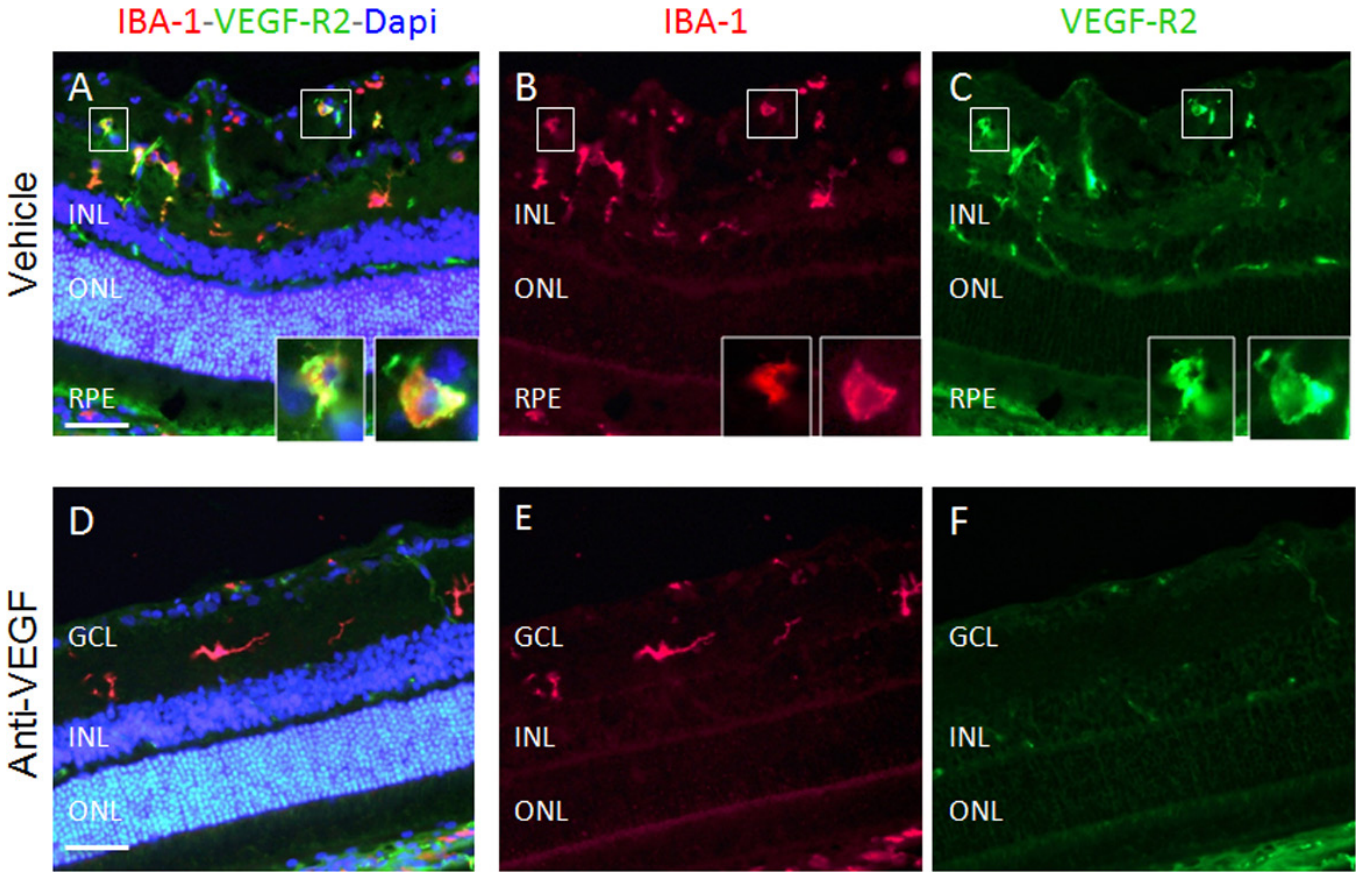

Figure 6. VEGF-R2 and IBA1 coimmunostaining on retinal sections retinal sections of EIU rats injected with vehicle (**A**–**C**) or anti-VEGF (**D**–**F**). GCL = ganglion cell layer, INL = inner nuclear layer, ONL = outer nuclear layer, RPE = retinal pigment epithelial cells, Chor = choroid. Insets are increased magnification (5X) of regions delimited by squares. Bar = 50 µm.

related to inhibition of angiogenesis. Whereas treatment with specific rat anti-VEGF antibodies reduces ocular VEGF levels, it does not significantly reduce inflammation clinically and biologically. Indeed, no significant decrease in the major cytokines involved in EIU was measured in the ocular media, and no significant decrease in infiltrating polymorphonuclear was observed after anti-VEGF treatment. However, reducing VEGF by neutralizing anti-VEGF antibodies decreased the activation state of the microglia and macrophages in the retina and the choroid, as shown by the decreased round amoeboid IBA1-positive cells and the decreased production of NOS2 by those cells. These effects were specific since the rat isotype IgG had no effect, demonstrating that anti-VEGF has direct modulating effects on the activation state of microglia and macrophages.

Previous work from our group demonstrated that macrophage and microglia depletion by liposomes containing dichloromethylene-diphosphonate decreased clinical signs of EIU but did not decrease cellular retinal infiltration [23]. Several reasons can explain this discrepancy. First, the route of injection of anti-VEGF antibody in the vitreous might not be optimal in this model of ocular inflammation that affects the anterior segment of the eye. Moreover, placental growth factor (PGF) that activated Flt-1 [46] is not neutralized by anti-VEGF antibody. This could explain that microglia and macrophages were partially deactivated as shown by the non-significant downregulation of TNF-α in the retina in the treated eyes. Another explanation could be that only a subset of microglia and macrophages express VEGF receptors suggesting that other factors could modulate their activation state. Moreover, deactivation of macrophages and microglia is not directly comparable to depletion of macrophages and microglia. The balance of pro- and anti-inflammatory mediators produced by macrophages and microglia probably regulates ocular inflammation in a more complex manner [47,48]. Finally, the local administration of anti-VEGF probably does not act on circulating monocytes since its systemic passage is low.

In our experiments, we cannot exclude that anti-VEGF also acted on infiltrating myeloid cells that are also labeled

by IBA1. However, the systemic depletion of circulating macrophages did not decrease the retinal cellular infiltration suggesting that circulating monoctyes and macrophages poorly contribute to inflammation in the posterior segment [23].

No animal model recapitulates all features of human diseases, but the fact that in a specific model of acute inflammation, anti-VEGF exerts direct effects on the activation of microglia and macrophages in the retina and the choroid suggests that similar effects could intervene in more complex retinal diseases where sub-clinical inflammation and microglial activation are suspected to be pathogenic. Clinical studies suggested that long-term anti-VEGF treatment for diabetic macular edema had an unexpected effect on the diabetic retinopathy severity [35]. Microglia deactivation by anti-VEGF could be a mechanism that mediates this beneficial effect. Novel anti-VEGF drugs such as aflibercept that neutralize VEGF and PGF might have potentiated activity on microglia activation. However, whether VEGF-induced microglia activation could have beneficial effects on clearance of retinal debris as shown for alveolar macrophages [49] remains to be evaluated, and whether full inhibition of microglia activation would be more beneficial in the retina remains unclear.

In conclusion, anti-VEGF drugs may exert significant unsuspected effects on retinal and choroidal microglia and macrophages that play important and complex roles in the pathogenesis of retinal diseases. Further studies should evaluate these effects in different ocular models of retinal diseases.

REFERENCES

1. Hickey WF, Kimura H. Perivascular microglial cells of the CNS are bone marrow-derived and present antigen in vivo. Science 1988; 239:290-2. [PMID: 3276004].
2. Perry VH, Gordon S. Macrophages and microglia in the nervous system. Trends Neurosci 1988; 11:273-7. [PMID: 2465626].
3. Streit WJ, Graeber MB, Kreutzberg GW. Functional plasticity of microglia: a review. Glia 1988; 1:301-7. [PMID: 2976393].
4. Lassmann H, Schmied M, Vass K, Hickey WF. Bone marrow derived elements and resident microglia in brain inflammation. Glia 1993; 7:19-24. [PMID: 7678581].
5. Ling EA, Wong WC. The origin and nature of ramified and amoeboid microglia: a historical review and current concepts. Glia 1993; 7:9-18. [PMID: 8423067].
6. Ling EA. Monocytic origin of ramified microglia in the corpus callosum in postnatal rat. Neuropathol Appl Neurobiol 1994; 20:182-3. [PMID: 8072651].
7. Zeng XX, Ng YK, Ling EA. Neuronal and microglial response in the retina of streptozotocin-induced diabetic rats. Vis Neurosci 2000; 17:463-71. [PMID: 10910112].
8. Zeng HY, Green WR, Tso MOM. Microglial activation in human diabetic retinopathy. Arch Ophthalmol 2008; 126:227-32. [PMID: 18268214].
9. Combadière C, Feumi C, Raoul W, Keller N, Rodéro M, Pézard A, Lavalette S, Houssier M, Jonet L, Picard E, Debré P, Sirinyan M, Deterre P, Ferroukhi T, Cohen SY, Chauvaud D, Jeanny JC, Chemtob S, Behar-Cohen F, Sennlaub F. CX3CR1-dependent subretinal microglia cell accumulation is associated with cardinal features of age-related macular degeneration. J Clin Invest 2007; 117:2920-8. [PMID: 17909628].
10. Rao NA, Kimoto T, Zamir E, Giri R, Wang R, Ito S, Pararajasegaram G, Read RW, Wu GS. Pathogenic role of retinal microglia in experimental uveoretinitis. Invest Ophthalmol Vis Sci 2003; 44:22-31. [PMID: 12506051].
11. Xu H, Chen M, Forrester JV. Para-inflammation in the aging retina. Prog Retin Eye Res 2009; 28:348-68. [PMID: 19560552].
12. Xu H, Chen M, Manivannan A, Lois N, Forrester JV. Age-dependent accumulation of lipofuscin in perivascular and subretinal microglia in experimental mice. Aging Cell 2008; 7:58-68. [PMID: 17988243].
13. Omri S, Behar-Cohen F, de Kozak Y, Sennlaub F, Verissimo LM, Jonet L, Savoldelli M, Omri B, Crisanti P. Microglia/macrophages migrate through retinal epithelium barrier by a transcellular route in diabetic retinopathy: role of PKCζ in the Goto Kakizaki rat model. Am J Pathol 2011; 179:942-53. [PMID: 21712024].
14. Gaucher D, Chiappore JA, Pâques M, Simonutti M, Boitard C, Sahel JA, Massin P, Picaud S. Microglial changes occur without neural cell death in diabetic retinopathy. Vision Res 2007; 47:612-23. [PMID: 17267004].
15. Kern TS. Contributions of inflammatory processes to the development of the early stages of diabetic retinopathy. Exp Diabetes Res 2007; 2007:95103-[PMID: 18274606].
16. Xu H, Chen M, Mayer EJ, Forrester JV, Dick AD. Turnover of resident retinal microglia in the normal adult mouse. Glia 2007; 55:1189-98. [PMID: 17600341].
17. Ma W, Zhao L, Fontainhas AM, Fariss RN, Wong WT. Microglia in the mouse retina alter the structure and function of retinal pigmented epithelial cells: a potential cellular interaction relevant to AMD. PLoS ONE 2009; 4:e7945-[PMID: 19936204].
18. Krady JK, Basu A, Allen CM, Xu Y, LaNoue KF, Gardner TW, Levison SW. Minocycline reduces proinflammatory cytokine expression, microglial activation, and caspase-3 activation in a rodent model of diabetic retinopathy. Diabetes 2005; 54:1559-65. [PMID: 15855346].
19. Zhang M, Xu G, Liu W, Ni Y, Zhou W. Role of fractalkine/CX3CR1 interaction in light-induced photoreceptor

degeneration through regulating retinal microglial activation and migration. PLoS ONE 2012; 7:e35446-[PMID: 22536384].

20. Lee YS, Amadi-Obi A, Yu C-R, Egwuagu CE. Retinal cells suppress intraocular inflammation (uveitis) through production of interleukin-27 and interleukin-10. Immunology 2011; 132:492-502. [PMID: 21294722].

21. McMenamin PG, Crewe J. Endotoxin-induced uveitis. Kinetics and phenotype of the inflammatory cell infiltrate and the response of the resident tissue macrophages and dendritic cells in the iris and ciliary body. Invest Ophthalmol Vis Sci 1995; 36:1949-59. [PMID: 7657537].

22. Yang P, de Vos AF, Kijlstra A. Macrophages in the retina of normal Lewis rats and their dynamics after injection of lipopolysaccharide. Invest Ophthalmol Vis Sci 1996; 37:77-85. [PMID: 8550337].

23. Pouvreau I, Zech JC, Thillaye-Goldenberg B, Naud MC, Van Rooijen N, de Kozak Y. Effect of macrophage depletion by liposomes containing dichloromethylene-diphosphonate on endotoxin-induced uveitis. J Neuroimmunol 1998; 86:171-81. [PMID: 9663563].

24. Grunin M, Hagbi-Levi S, Chowers I. The role of monocytes and macrophages in age-related macular degeneration. Adv Exp Med Biol 2014; 801:199-205. [PMID: 24664699].

25. Sawano A, Iwai S, Sakurai Y, Ito M, Shitara K, Nakahata T, Shibuya M. Flt-1, vascular endothelial growth factor receptor 1, is a novel cell surface marker for the lineage of monocyte-macrophages in humans. Blood 2001; 97:785-91. [PMID: 11157498].

26. Forstreuter F, Lucius R, Mentlein R. Vascular endothelial growth factor induces chemotaxis and proliferation of microglial cells. J Neuroimmunol 2002; 132:93-8. [PMID: 12417438].

27. Norazit A, Nguyen MN, Dickson CG, Tuxworth G, Goss B, Mackay-Sim A, Meedeniya AC. Vascular endothelial growth factor and platelet derived growth factor modulates the glial response to a cortical stab injury. Neuroscience 2011; 192:652-60. [PMID: 21704679].

28. Ryu JK, Cho T, Choi HB, Wang YT, McLarnon JG. Microglial VEGF receptor response is an integral chemotactic component in Alzheimer's disease pathology. J Neurosci 2009; 29:3-13. [PMID: 19129379].

29. Dhoot DS, Kaiser PK. Ranibizumab for age-related macular degeneration. Expert Opin Biol Ther 2012; 12:371-81. [PMID: 22309606].

30. Ohr M, Kaiser PK. Aflibercept in wet age-related macular degeneration: a perspective review. Ther Adv Chronic Dis 2012; 3:153-61. [PMID: 23342231].

31. Browning DJ, Kaiser PK, Rosenfeld PJ, Stewart MW. Aflibercept for age-related macular degeneration: a game-changer or quiet addition? Am J Ophthalmol 2012; 154:222-6. [PMID: 22813448].

32. Campochiaro PA. Anti-vascular endothelial growth factor treatment for retinal vein occlusions. Ophthalmologica 2012; 227:Suppl 130-5. [PMID: 22517123].

33. Ho AC, Scott IU, Kim SJ, Brown GC, Brown MM, Ip MS, Recchia FM. Anti-vascular endothelial growth factor pharmacotherapy for diabetic macular edema: a report by the American Academy of Ophthalmology. Ophthalmology 2012; 119:2179-88. [PMID: 22917890].

34. Zechmeister-Koss I, Huic M. Vascular endothelial growth factor inhibitors (anti-VEGF) in the management of diabetic macular oedema: a systematic review. Br J Ophthalmol 2012; 96:167-78. [PMID: 22133986].

35. Ip MS, Domalpally A, Hopkins JJ, Wong P, Ehrlich JS. Long-term effects of ranibizumab on diabetic retinopathy severity and progression. Arch Ophthalmol 2012; 130:1145-52. .

36. Rosenbaum JT, McDevitt HO, Guss RB, Egbert PR. Endotoxin-induced uveitis in rats as a model for human disease. Nature 1980; 286:611-3. [PMID: 7402339].

37. Wang AL, Yu AC, Lau LT, Lee C. Wu le M, Zhu X, Tso MO. Minocycline inhibits LPS-induced retinal microglia activation. Neurochem Int 2005; 47:152-8. .

38. Bousquet E, Zhao M, Ly A, Leroux Les Jardins G, Goldenberg B, Naud MC, Jonet L, Besson-Lescure B, Jaisser F, Farman N, De Kozak Y, Behar-Cohen F. The aldosterone-mineralocorticoid receptor pathway exerts anti-inflammatory effects in endotoxin-induced uveitis. PLoS ONE 2012; 7:e49036-.

39. Ohsawa K, Imai Y, Sasaki Y, Kohsaka S. Microglia/macrophage-specific protein Iba1 binds to fimbrin and enhances its actin-bundling activity. J Neurochem 2004; 88:844-56. Available at[PMID: 14756805].

40. Miller JW, Le Couter J, Strauss EC, Ferrara N. Vascular endothelial growth factor a in intraocular vascular disease. Ophthalmology 2013; 120:106-14. [PMID: 23031671].

41. Shibuya M. Vascular endothelial growth factor and its receptor system: physiological functions in angiogenesis and pathological roles in various diseases. J Biochem 2013; 153:13-9. [PMID: 23172303].

42. Murakami M, Iwai S, Hiratsuka S, Yamauchi M, Nakamura K, Iwakura Y, Shibuya M. Signaling of vascular endothelial growth factor receptor-1 tyrosine kinase promotes rheumatoid arthritis through activation of monocytes/macrophages. Blood 2006; 108:1849-56. .

43. Barleon B, Sozzani S, Zhou D, Weich HA, Mantovani A, Marmé D. Migration of human monocytes in response to vascular endothelial growth factor (VEGF) is mediated via the VEGF receptor flt-1. Blood 1996; 87:3336-43. .

44. Choi JS, Kim HY, Cha JH, Choi JY, Park SI, Jeong CH, Jeun SS, Lee MY. Upregulation of vascular endothelial growth factor receptors Flt-1 and Flk-1 following acute spinal cord contusion in rats. J Histochem Cytochem 2007; 55:821-30. .

45. Lemaitre C, Thillaye-Goldenberg B, Naud MC, De Kozak Y. The effects of intraocular injection of interleukin-13 on endotoxin-induced uveitis in rats. Invest Ophthalmol Vis Sci 2001; 42:2022-30. [PMID: 11481267].

46. Autiero M, Waltenberger J, Communi D, Kranz A, Moons L, Lambrechts D, Kroll J, Plaisance S, De Mol M, Bono F, Kliche S, Fellbrich G, Ballmer-Hofer K, Maglione D, Mayr-Beyrle U, Dewerchin M, Dombrowski S, Stanimirovic D, Van Hummelen P, Dehio C, Hicklin DJ, Persico G, Herbert JM, Communi D, Shibuya M, Collen D, Conway EM, Carmeliet P. Role of PlGF in the intra- and intermolecular cross talk between the VEGF receptors Flt1 and Flk1. Nat Med 2003; 9:936-43. .

47. Broderick C, Duncan L, Taylor N, Dick AD. IFN-gamma and LPS-mediated IL-10-dependent suppression of retinal microglial activation. Invest Ophthalmol Vis Sci 2000; 41:2613-22. [PMID: 10937574].

48. Kearns MT, Dalal S, Horstmann SA, Richens TR, Tanaka T, Doe JM, Boe DM, Voelkel NF, Taraseviciene-Stewart L, Janssen WJ, Lee CG, Elias JA, Bratton D, Tuder RM, Henson PM, Vandivier RW. Vascular endothelial growth factor enhances macrophage clearance of apoptotic cells. Am J Physiol Lung Cell Mol Physiol 2012; 302:L711-8. .

49. Chen L, Yang P, Kijlstra A. Distribution, markers, and functions of retinal microglia. Ocul Immunol Inflamm 2002; 10:27-39. [PMID: 12461701].

Articles are provided courtesy of Emory University and the Zhongshan Ophthalmic Center, Sun Yat-sen University, P.R. China. The print version of this article was created on 23 June 2014. This reflects all typographical corrections and errata to the article through that date. Details of any changes may be found in the online version of the article.